

Dislocation Reduction by Glide in Epitaxial IV–VI Layers on Si Substrates

H. ZOGG^{1,2}

1.—Thin Film Physics Group, ETH Zurich, 8005 Zurich, Switzerland. 2.—e-mail: zogg@phys.ethz.ch

It is explained with a simple model why the reduction of threading dislocation (TD) densities in epitaxial lattice and thermal expansion mismatched IV–VI layers such as PbSe(111) on Si(111) substrates follows a $1/h^2$ dependence where h is the thickness of the layer. This is in contrast to the $1/h$ dependence for III–V and II–VI layers grown on mismatched substrates. The $1/h^2$ dependence results since the thermal mismatch strain is mainly reduced by glide and reactions of the TD in their main {100}-type glide system of the NaCl-type IV–VI semiconductors. In addition, multiple thermal cycles lead to further reduction of the TD densities by glide and fusion since fusion does not cause dislocation blocking.

Key words: Molecular beam epitaxy, heteroepitaxy, dislocation reduction, lead chalcogenides

INTRODUCTION

Reduction of threading dislocation (TD) densities in lattice-mismatched growth of semiconductor layers remains as an important issue since the beginning of the development of molecular beam epitaxy (MBE) techniques. Unfortunately, misfit dislocations (MD) formed during growth to overcome the lattice mismatch at the interface between layer and substrate do not remain at the interface over the whole sample size, but bend up after a certain length and cross the layer towards the surface, thus forming threading ends (TD). Elimination or at least drastic reduction of these TD densities is of utmost importance to get device-quality layers. Since only the topmost part of the semiconductor material is electrically active in typical electronic devices, the threading dislocation density at the surface mainly determines possible deteriorations of the performance of the devices. The dislocation density near the interface (as well as the mean dislocation density in the layer) is not of importance in this context.

The density of TD decreases with increasing layer thickness already during the MBE process. If two

TD approach within a reaction distance during the growth of the layer, they may annihilate if their Burgers vectors allow it. If $\rho(y)$ is the areal density of TD in the layer at distance y from the interface, the recombination of the TD is proportional to $\rho(y)^2$. Therefore, for this binary recombination,

$$\frac{d\rho}{dy} = -c_1\rho^2. \quad (1)$$

At the surface of a layer of total thickness h ($y = h$) this results in a $\rho \propto 1/h$ dependence.¹ For very thick layers, i.e., very low dislocation densities, one-dislocation reactions become important too, leading to a somewhat more generalized reaction equation of

$$\frac{d\rho}{dy} = -c_1\rho^2 - c_2\rho, \quad (2)$$

where c_1 and c_2 are constants.² This leads to an exponential decrease at large thicknesses h where the first term becomes negligible. This transition occurred above a thickness of $\sim 70 \mu\text{m}$ for GaAs on Si.² Here, the initial density of TD was around 10^9 cm^{-2} , while it decreased to $\sim 10^6 \text{ cm}^{-2}$ above $100 \mu\text{m}$ thickness. However, such large thicknesses are rather impractical for device applications.

(Received November 5, 2011; accepted February 20, 2012; published online March 16, 2012)

The same behavior was observed for CdTe(211) on Ge substrates where TD densities $\rho \approx 5 \times 10^6 \text{ cm}^{-2}$ were reached at 10 μm layer thickness.³

For HgCdTe(211) layers on Si(211) substrates, a somewhat similar but more extended analysis was recently presented.⁴ Dislocation densities of 10^6 cm^{-2} were reached. The authors note that multiple thermal cyclic anneals (TCA) are more effective to decrease the TD densities than just single anneals.⁵ This means that the glide of TD becomes most important. This is caused by the stress fields on changes of temperatures due to the thermal mismatch between II–VI materials and Si. However, such reactions may lead to sessile dislocations, which hinder further TD reduction so that the TD density saturates at a $\sim 10^6 \text{ cm}^{-2}$ level. Dislocation reactions in zincblende-type strained epitaxial layers have been analyzed in detail.⁶ Some of the reactions lead to blocking of the TD, which impedes further reductions.

DISLOCATION REDUCTION IN EPITAXIAL IV–VI LAYERS

For IV–VI layers, such as PbSe or PbTe on Si(111) substrates, the situation is different. TCA is well known to efficiently decrease TD densities. This is due to the huge thermal expansion mismatch and the extremely easy glide of TD in the layers.^{7–12} Here, a $\rho \propto 1/h^2$ dependence was observed,⁷ but only partially explained. This dependence is not described by the models above. It is the purpose of this communication to give a better explanation of the $1/h^2$ dependence, which, of course, is favorable for reduction of TD, and, in addition, to discuss the limits of TCA in obtaining the lowest TD densities.

Note that a $1/h^2$ dependence was described for Ge and GaAs on Si(100) by Wang et al.¹³ and explained to describe the *equilibrium minimal* TD density after high-temperature anneal.

The narrow-gap IV–VI (lead chalcogenide) semiconductors crystallize in the NaCl structure, contrary to the zincblende-type III–V and II–VI materials. The main glide planes of IV–VIs are of {100} type (while they are {111} for zincblende structures). The Burgers vectors are of $a/2\langle 110 \rangle$ type for both cases. Device-quality (111)-oriented IV–VI layers of up to several microns thickness are obtained on Si(111) substrates. Keeping in mind that the thermal expansion coefficient of IV–VI ($\alpha \approx 2 \times 10^{-5} \text{ K}^{-1}$ at RT) is about 7 times larger compared with that of Si, it is surprising that such thick layers do not crack when cooling down from the MBE growth temperature ($\sim 400^\circ\text{C}$) to room temperature (RT), or even cryogenic temperatures where infrared detectors work. The strain which develops during MBE growth due to the lattice mismatch and due to the thermal mismatch when cooling down to RT *as well as on each temperature change after growth* is nearly completely relaxed due to glide of dislocations on the main {100}-type glide planes.¹⁰ These planes are arranged in three-fold symmetry in (111)-oriented layers. Most importantly, they are inclined by 54° to the surface. Thus, glide is allowed since their Schmid factor is not zero. Glide is extremely easy in many high-quality epitaxial IV–VI layers; the materials are soft. The softness is not of importance for applications if the layers are grown on a rigid substrate such as Si. Mid-infrared detector focal-plane arrays as well as mid-infrared vertical external cavity surface-emitting lasers (VECSEL) have been realized on Si(111) substrates.^{14–16} In contrast, when grown on Si(100) substrates, layers thicker than about 0.5 μm typically crack since thermal mismatch strain cannot relax, as the {100} main glide planes are parallel or perpendicular to the surface with zero Schmid factor.¹¹

Figure 1 shows the arrangement with threefold symmetry for a (111)-oriented IV–VI layer on

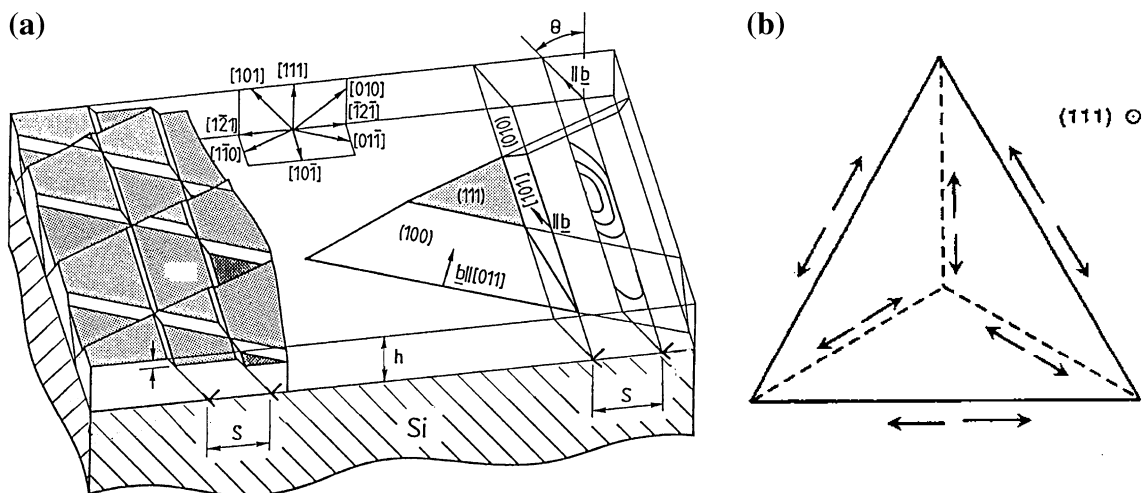


Fig. 1. Schematic drawing of the {100}⟨110⟩ glide system for NaCl-type IV–VI(111) layers on Si(111): (a) perspective drawing, and (b) $a/2\langle 110 \rangle$ -type Burgers vectors inclined (dashed, glissile dislocations) and parallel (full lines, sessile dislocations) to the interface.^{7,10}

Si(111) during or after strain relaxation. A terraced structure results with a height difference of the individual terraces of one or several perpendicular components of the Burgers vectors. Once a misfit part (MD) has formed during growth or after a temperature change [as indicated in the (010) plane at the right side of the perspective drawing], both threading ends (TD) of this dislocation extending to the surface may glide in the (010) plane. This leads to a strain relaxation perpendicular to the intercept of this plane with the substrate, i.e., in the [121] direction. It was found that such TD move back and forth many times on each temperature change. Total cumulative glide lengths of several centimeters were observed after >1000 temperature cycles between RT and 77 K.¹⁰

When cycling between RT and 300°C, the density of TDs decreased from $\sim 10^8 \text{ cm}^{-2}$ to $\sim 10^6 \text{ cm}^{-2}$ after 15 cycles for high-quality PbSe layers of a few microns thickness (Fig. 2).^{8,9} The decrease follows a power law $(1 - c)^n$ where n is the number of cycles and $c \approx 0.2$ for the present case. From this value, information on the reaction radius may be obtained.⁸ The density of TD decreased slightly even when cycling between RT and 77 K.

DISLOCATION DENSITIES VERSUS LAYER THICKNESS IF GLIDE IS IMPORTANT

Interestingly, the density of TDs (etch pit density) after at least one temperature cycle decreases with a $1/h^2$ behavior. This is shown in Fig. 3 (from Ref. 7) for PbSe samples with thicknesses h ranging from $\sim 0.5 \mu\text{m}$ to $4 \mu\text{m}$. The details of the preparation of the samples (etch thinning followed by anneal) is described in Ref. 7). The $1/h^2$ decrease may be explained as follows:

We assume binary recombination. The areal density of TD at the surface of a layer of thickness h

is $\rho(h)$. When changing the temperature, the TD glide in order to relax the thermal mismatch strain. If the temperature change is large enough that the gliding TD encounters another TD, we assume that these two TD which cross or meet within the reaction distance fuse or annihilate with a certain probability if their Burgers vectors allow it (see below). This reaction may occur anywhere across the layer thickness. Since the glide planes are inclined with respect to the surface, the width which is swept by the gliding TD is $h \tan\theta$, i.e., the projection of the glide plane onto the interface plane. It is proportional to the thickness h . Therefore,

$$\frac{d\rho}{dh} = -c_3 h \rho^2, \quad (3)$$

where c_3 is a constant. This is different by a factor of h compared with Eq. 1, where no glide was considered.

The solution is

$$\rho = \rho_0 \left(1 + \frac{c_3 h^2}{2}\right)^{-1}, \quad (4)$$

where ρ_0 is the initial dislocation density near the interface. For thicknesses of interest in the present work one may neglect the 1 in the denominator. This leads to the

$$\rho \propto \frac{1}{h^2} \quad (5)$$

dependence as experimentally observed. The thicker the layer, the larger the area swept by the glide, leading to a stronger than $\rho \propto 1/h$ decrease. Note that this stronger, $1/h^2$ decrease needs glide of TD (which extend up to the surface of the layer) by a suitable force. It is assumed that this force is mainly induced by the thermal mismatch on temperature change. The temperature change may be the cooling of the sample from growth to room temperature, or a separate anneal after growth. The equation does not

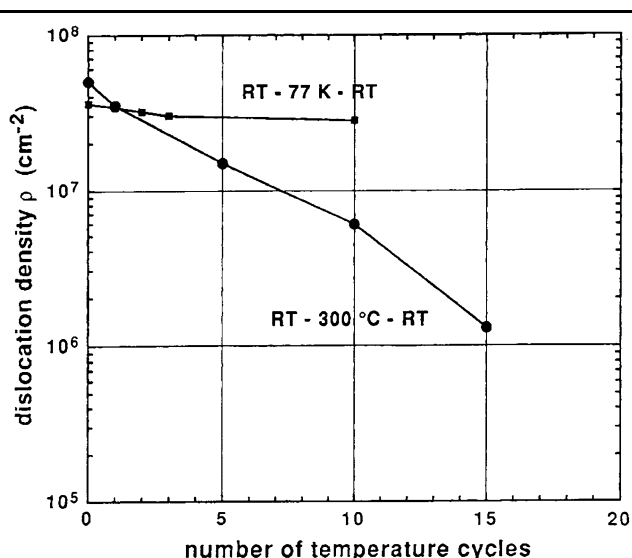


Fig. 2. Decrease of etch pit density versus number of thermal anneal cycles to 300°C and to 77 K.⁹

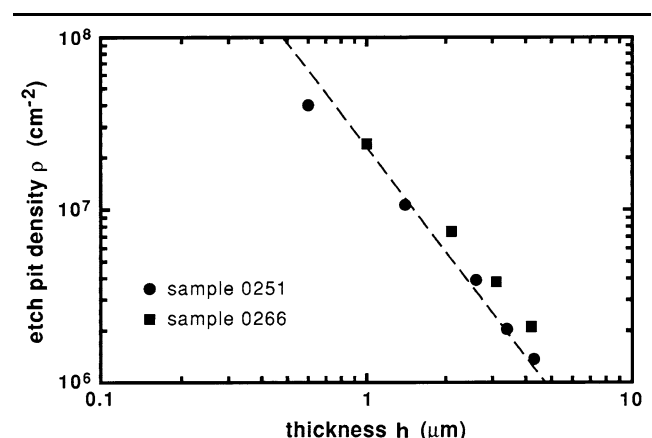


Fig. 3. Etch pit density in PbSe(111) on Si(111) versus thickness h of the layer. The dashed line indicates a $1/h^2$ dependence.⁷

necessarily apply *during* the MBE growth with the sample held at constant growth temperature.

DISLOCATION REACTIONS AND SWEEP LENGTHS

It remains to show: (I) which dislocation reactions occur and which may lead to sessile dislocations no longer helping by glide to reduce the density of the TD, and (II) how long a TD has to sweep in order to encounter a second TD, i.e., which are the lowest densities which can be achieved in practice for reasonable substrate sizes.

As regards point I, there are 12 Burgers vectors b of $a/2\langle 110 \rangle$ type, as plotted in Fig. 1b. From these, six are inclined with respect to the surface of the layer, thus leading to glissile (g) TD. The remaining six Burger vectors b are parallel to the surface, and therefore TD with these b are sessile (s). Fusion of two TD (of which at least one is glissile) with non-parallel Burgers vector b_1 and b_2 occurs if the resulting Burgers vector $b_3 = b_1 + b_2$ is again of $a/2\langle 110 \rangle$ type. Analyzing the possible fusion reactions according to Fig. 1b, one finds that a glissile (g) and a sessile (s) TD may fuse to a new glissile (g) one: $g + s \rightarrow g$. There are also reactions of type $g + g \rightarrow s$. This is shown schematically in Fig. 4a, too.⁷ However, this new sessile (s) TD may react again with a glissile (g) TD according to the first reaction. Therefore, there are always glissile (g) TD available for further TD reduction. Therefore, with each TCA, the TD density should decrease, and there is no lower limit with this model. Annihilation of two TD by glide may occur too, if their Burgers vectors are antiparallel and both TD run on parallel glide planes separated by a very small distance only to allow the reaction (Fig. 4b).

Considering point II, one has to estimate the mean free path of a TD and the glide length due to strain relaxation on a temperature change. The distance s between MD running parallel along the interface needed to relax the lattice mismatch strain (there are three such sets because of the threefold symmetry) is given by the lattice mismatch ε and $b_{\text{eff}} = b \sin \theta$, the projection of the length of the Burgers vector onto the interface plane,

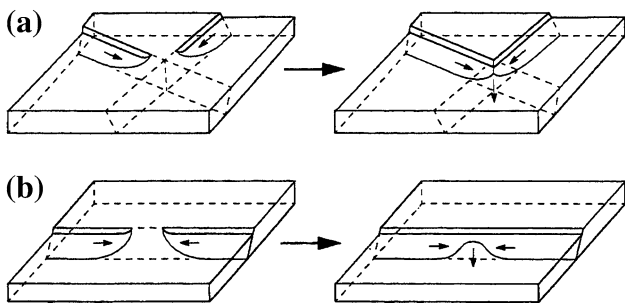


Fig. 4. Glide of two TD on differently oriented glide planes leading to fusion (a); glide of two TD on the same glide plane leading to annihilation (b).¹¹

$s = 3/2b_{\text{eff}}\varepsilon^{-1}$. The MD do not run along the whole sample size and end at the edge. Rather, they have a mean length L and are terminated at both ends by TD segments bending up and ending at the surface of the layer (Fig. 5 for one of the three sets). It follows from geometry [for (111) orientation¹⁰] that $sL\rho = 6$.

Since we are interested only in the additional MD lengths L' caused by the thermal expansion mismatch, we may use a value $\varepsilon = 0.006$ for a temperature change of 300 K for the anneals (the difference of the thermal expansion coefficient between PbSe and Si is $\sim 2 \times 10^{-5} \text{ K}^{-1}$).

For PbSe with $b = 0.43 \text{ nm}$ and $\varepsilon = 0.006$ a distance $s = 63 \text{ nm}$ is calculated. For TD density $\rho = 10^8 \text{ cm}^{-2}$, the length change is $L' = 100 \mu\text{m}$, while for $\rho = 10^6 \text{ cm}^{-2}$, L' is as long as $L' = 10 \text{ mm}$.

The mean free path λ that a TD can glide until it encounters another TD is given by the swept area (projection of the glide plane onto the surface) $\lambda h \text{tg}\theta = 1/\rho$. Values for $\rho = 10^8 \text{ cm}^{-2}$ and $\rho = 10^6 \text{ cm}^{-2}$ are $\lambda = 2 \mu\text{m}$ and $\lambda = 200 \mu\text{m}$, respectively, for a PbSe layer of thickness $h = 1 \mu\text{m}$. The ratio $L'/\lambda = 4ch/b \cos \theta \approx 50$ is independent of ρ for the examples given.

Therefore, the mean free path λ is always much shorter than the length swept by the TD for these conditions, and the density of TD by TCA should continue to decrease to any low value. However, if λ exceeds the dimension of the sample, the reduction of the TDs will diminish.

In practice, a lowest value of $\rho \approx 10^6 \text{ cm}^{-2}$ was reproducibly achieved for high-quality samples.

However, for samples with small sizes, or samples containing "macroscopic" defects (possibly wrongly oriented nuclei), the minimal densities ρ were higher or even increased from a minimal value when applying still more temperature cycles. The same was found for a doped PbTe:Bi sample.⁸ Therefore, other TD blocking mechanisms are active in these samples.

The present limit of $\rho \approx 10^6 \text{ cm}^{-2}$ may be further reduced with improved MBE techniques leading to layers with improved structural quality with still fewer defects. Growth interruptions with temperature

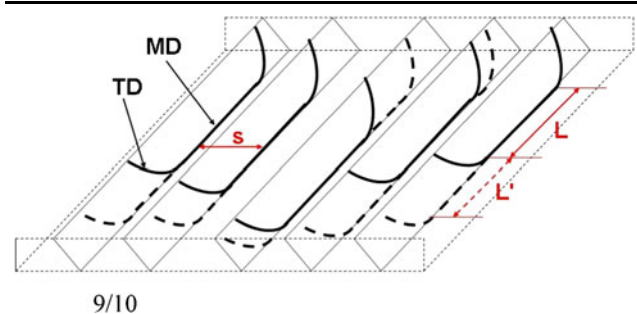


Fig. 5. MD and TD segments in one of the three equivalent $\{100\}$ -type glide planes. The mean spacing s between the MD is given by the mismatch, while the mean length L and L' of the MD segments are inversely proportional to the areal density ρ of the TD.

cycling of the substrate during these interruptions are an attempt to improve layer quality.

However, in addition to TD in the main $\{100\}\langle 110\rangle$ glide systems, there may be a few TD belonging to other glide systems and other sessile dislocations which are not eliminated by the dislocation fusions described above even in high-quality samples. Comparing λ with L' even after many TCA, a ratio below $1:10^5$ was estimated that crossing TD give rise to a blocking.¹² Such TD may limit the lowest densities achievable even in otherwise perfect samples.

Ueta et al.¹⁷ found a $\rho \propto 1/h^{1.2}$ dependence for PbTe layers grown on BaF₂(111). The thermal expansion coefficients of PbTe and BaF₂ are nearly the same. The $1/h^{1.2}$ dependence may therefore be qualitatively explained to be caused by some glide effects of TD during growth because of the lattice mismatch, while the thermal expansion mismatch is negligible.

INFLUENCE OF DISLOCATIONS ON ELECTRONIC PROPERTIES

As already mentioned, applications of epitaxial IV–VI layers on Si(111) realized include infrared detector arrays as well as VECSELs. The performance of these devices is limited in most cases due to the defects created by the TD. The mean distance between two such TD is D_{TD} . The low-temperature saturation Hall mobilities μ_{sat} are limited by D_{TD} . A rough correlation between this distance $D_{TD} = 1/\sqrt{\rho}$, the performance (resistance–area product R_0A) of photovoltaic IR detectors, and Shockley–Read carrier lifetime τ_{sr} is observed as^{14–16}

$$\mu_{sat} \propto \frac{1}{\sqrt{\rho}}, \quad \text{and} \quad \tau_{sr} \propto R_0A \propto \frac{1}{\rho}.$$

This correlates the threading dislocation densities with electronic properties of the devices.

However, IV–VI materials have been much less investigated than other compound semiconductors such as III–V or II–VI materials. There is nearly no information on how dislocations in IV–VI heteroepitaxial layers nucleate. It was never observed that the quality of the IV–VI layers or devices is influenced by a slight miscut (up to a few degrees) of the Si(111) substrates. Details on the interplay between TD and device properties, e.g., whether sessile TD are more detrimental than glissile TD, are not known.

Further applications of IV–VI semiconductors include thermoelectric devices. The same arguments on TD density reduction apply for such epitaxial thin films on mismatched substrates^{18,19}

One might note that IV–VIs are quite unique within the other well-known semiconductors. This includes their special band structure (band extrema at the L points, nearly symmetric valence and conduction bands), and the extremely high permittivities. In this work, the mechanical properties

were mainly addressed, however. The softness of the IV–VI materials together with their NaCl structure leads to dislocation reactions which improve the structural quality of the layers. To the best knowledge of the author, such behavior is not observed in any other semiconducting material families.

CONCLUSIONS

It was shown that reduction of threading dislocation (TD) densities ρ in epitaxial lattice and thermal expansion mismatched IV–VI layers on Si(111) substrates follows a $\rho \propto 1/h^2$ dependence where h is the thickness of the layer, and explained by a simple model. The square dependence results since the thermal mismatch strain is mainly reduced by glide of the TD in their main $\{100\}$ -type glide system (inclined to the surface) before they react. This dependence is stronger than the $\rho \propto 1/h$ TD reduction valid for zincblende-type III–V and II–VI layers grown on lattice-mismatched substrates.

REFERENCES

1. H. Kroemer, T.-Y. Liu, and P.M. Petroff, *J. Cryst. Growth* 95, 96 (1989).
2. M. Tachikawa and M. Yamaguchi, *Appl. Phys. Lett.* 56, 484 (1990).
3. G. Badano, P. Gergaud, I.C. Robin, X. Baudry, B. Amstatt, and Frédérique. Gemain, *J. Electron. Mater.* 39, 908 (2010).
4. J.D. Benson, S. Farrell, G. Brill, Y. Chen, P.S. Wijewarnasuriya, L.O. Bubulac, P.J. Smith, R.N. Jacobs, J.K. Markunas, M. Jaime-Vasquez, L.A. Almeida, A. Stoltz, U. Lee, M.F. Vilela, J. Peterson, S.M. Johnson, D.D. Lofgreen, D. Rhiger, E.A. Patten, and P.M. Goetz, *J. Electron. Mater.* 40, 1847 (2011).
5. S. Farrell, G. Brill, Y.P. Chen, P.S. Wijewarnasuriya, M.V. Rao, N. Dhar, and K. Harris, *J. Electron. Mater.* 39, 43 (2010).
6. J.S. Speck, M.A. Brewer, G. Beltz, A.E. Romanov, and W. Pompe, *J. Appl. Phys.* 80, 3808 (1996).
7. P. Müller, H. Zogg, A. Fach, J. John, C. Paglino, A.N. Tiwari, M. Krejci, and G. Kosterz, *Phys. Rev. Lett.* 78, 3007 (1997).
8. H. Zogg, K. Alchalabi, and D. Gössi, *Proc. 9th Int. Conf. on Narrow Gap Semiconductors (NG9)*, ed. N. Puhlmann, H.-U. Müller, and M. von Ortenberg (Humboldt University at Berlin, Germany, 1999).
9. H. Zogg and J. John, *Opto-Electron. Rev.* 6, 37 (1998).
10. H. Zogg, S. Blunier, A. Fach, C. Maissen, P. Müller, S. Teodoropol, V. Meyer, G. Kosterz, A. Dommann, and T. Richmond, *Phys. Rev. B* 50, 10801 (1994).
11. P. Müller (Ph.D. thesis, ETH Nr. 12011, 1997).
12. P. Müller, A. Fach, J. John, J. Masek, C. Paglino, and H. Zogg, *Appl. Surf. Sci.* 102, 130 (1996).
13. G. Wang, R. Loo, E. Simoen, L. Souriau, M. Caymax, M.M. Heyns, and B. Blanpain, *Appl. Phys. Lett.* 94, 102115 (2009).
14. H. Zogg, K. Alchalabi, D. Zimin, and K. Kellermann, *IEEE Trans. Electron Dev.* 50, 209 (2003).
15. H. Zogg, M. Arnold, F. Felder, M. Rahim, C. Ebnetter, I. Zasavitskiy, N. Quack, S. Blunier, and J. Dual, *J. Electron. Mater.* 37, 1497 (2008).
16. M. Rahim, A. Khair, M. Fill, F. Felder, and H. Zogg, *Electron. Lett.* 47, 1037 (2011).
17. A.Y. Ueta, G. Springholz, and G. Bauer, *J. Cryst. Growth* 175/176, 1022 (1997).
18. H. Böttner, G. Chen, and R. Venkatasubramanian, *MRS Bull.* 31, 211 (2006).
19. J. Nurnus, J. John, and H. Griessmann, *Proceedings 4th European Workshop on Thermoelectrics (Madrid, 1998)*.